

Optical spin transport theory of spin-1/2 topological Fermi superfluids

Hiroyuki Tajima,¹ Yuta Sekino,^{2,3} and Shun Uchino^{4,5}

¹*Department of Physics, Graduate School of Science,
The University of Tokyo, Tokyo 113-0033, Japan*

²*Quantum Hadron Physics Laboratory, RIKEN Nishina Center (RNC), Wako, Saitama, 351-0198, Japan*

³*Interdisciplinary Theoretical and Mathematical Sciences Program (iTHEMS), RIKEN, Wako, Saitama 351-0198, Japan*

⁴*Advanced Science Research Center, Japan Atomic Energy Agency, Tokai, Ibaraki 319-1195, Japan*

⁵*Waseda Institute for Advanced Study, Waseda University, Shinjuku, Tokyo 169-8050, Japan*

(Dated: February 9, 2022)

We theoretically investigate optical (frequency-dependent) bulk spin transport properties in a spin-1/2 topological Fermi superfluid. We specifically consider a one-dimensional system with an interspin p -wave interaction, which can be realized in ultracold atom experiments. Developing the BCS-Leggett theory to describe the Bardeen-Cooper-Schrieffer (BCS) to Bose-Einstein condensate (BEC) evolution and the \mathbb{Z}_2 topological phase transition in this system, we show how the spin transport reflects these many-body aspects. We find that the optical spin conductivity, which is a small AC response of a spin current, shows the spin gapped spectrum in the wide parameter region and the gap closes at \mathbb{Z}_2 topological phase transition point. Moreover, the validity of the low-energy effective model of the Majorana zero mode is discussed along the BCS-BEC evolution in connection with the scale invariance at p -wave unitarity.

I. INTRODUCTION

Topological superconductors and superfluids have accepted special interests from broad communities of modern physics¹. Phenomena emerging in topological matter such as liquid helium², unconventional superconductors³, 3P_2 neutron superfluids⁴, and color superconductors⁵ manifest fascinating properties relevant to cutting-edge quantum technology. For instance, Majorana fermions anticipated to appear at the edge of topological systems are crucial key ingredients for topological quantum computation⁶.

A spin transport plays a crucial role in revealing topological properties in condensed matter systems such as topological insulators¹ and spin Hall systems⁷, where the gapless edge state involves the helical spin transport with the time-reversal symmetry⁸. In particular, properties of AC spin transport provide us with intriguing opportunities to reveal non-trivial aspects of these systems and their application to spintronics⁹. In condensed matter, however, spin transport in mesoscale or submicron scale is manipulated^{10–20}, and exploration of bulk spin transport in a topological state of matter remains challenging. In Ref.²¹, we have recently pointed out that the optical (frequency-dependent) spin conductivity can be measured in ultracold atomic gases being ideal quantum simulators of condensed matter systems^{22–24}. Since the optical (charge) conductivity spectra have already been measured in an optical lattice system by using the similar method²⁵, detailed examinations of AC spin transport with cold-atom experiments get within reach.

Regarding the realization of topological superfluids in ultracold atomic gases, a p -wave superfluid Fermi gas has been one of the promising candidates for the past few decades^{26–28}. However, various effects such as three-body loss and dipolar relaxation^{29–35} prevent the systems from reaching the superfluid state. At the same time, it

has recently been suggested that such atom loss processes may be suppressed in the low-dimensional systems^{36–39}. Shortly afterwards, the corresponding atomic loss measurements in one-dimensional (1D) systems near the p -wave Feshbach resonance have been performed in several experimental groups^{40,41}. In this regard, a 1D spin-1/2 Fermi gas with an interspin p -wave interaction^{42,43} is one of the possible targets for realizing a topological Fermi superfluid because its three-body losses are weak compared to the fully spin polarized case, where the Bose-Fermi duality weakens the Pauli blocking effect in coordinate space at low energy scale^{44–53}. More explicitly, while a strong p -wave attraction induces the three-body collision by overwhelming the Pauli-blocking effect in fully polarized case, the Pauli-blocking between two identical fermions can suppress the three-body collision in the present spin-balanced mixture with only interspin interaction. In addition, the optical spin transport in interacting spin-1/2 systems can be non-trivial even in the absence of a lattice and impurities²¹. It is in contrast to fully spin polarized fermions, whose optical spin conductivity becomes independent of interatomic interactions due to the generalized Kohn's theorem⁵⁴. Moreover, the 1D p -wave Fermi gas at unitarity, where a p -wave scattering length diverges, shows the so-called universal thermodynamics⁵⁵ which makes thermodynamic quantities independent of any length scale associated with the interaction in spite of the presence of strong correlations^{43,46,47,49–53}. Thus, one can investigate a unique interplay between topological and universal aspects of this system, which has never been addressed yet.

Being motivated by these backgrounds, we discuss spin transport properties of a 1D unpolarized spin-1/2 p -wave superfluid Fermi gas at zero temperature. To this end, we develop the BCS-Leggett theory that allows to describe the BCS-BEC evolution and the topological phase transition in this system. Using the linear response the-

ory, moreover, we clarify how the optical spin transport properties reflect these non-trivial many-body effects by changing the p -wave interaction strength.

In Sec. II, we present the formalism of the BCS-Leggett theory and explain topological properties of this system. In Sec. III, we discuss the analytical properties of optical spin transport. In Sec. IV, we show the numerical results of bulk thermodynamics and the optical spin conductivity, and discuss the low-energy effective model for the Majorana zero mode. In Sec. V, we summarize this paper. In what follows, we take $\hbar = k_B = 1$ and the system size L is taken to be unity.

II. THEORETICAL MODEL

A. Hamiltonian

The Hamiltonian for a 1D unpolarized spin-1/2 Fermi gas with interspin p -wave interaction is given by

$$H = H_0 + V, \quad (1)$$

where

$$H_0 = \sum_{k,\sigma} \xi_k c_{k,\sigma}^\dagger c_{k,\sigma} \quad (2)$$

and

$$V = U \sum_{k,k',q} \Gamma_k \Gamma_{k'} c_{k+q/2,\uparrow}^\dagger c_{-k+q/2,\downarrow}^\dagger c_{-k'+q/2,\downarrow} c_{k'+q/2,\uparrow} \quad (3)$$

are the kinetic term and the p -wave interaction term that is assumed to be separable, respectively. In Eq. (2), $\xi_k = k^2/(2m) - \mu$ is the kinetic energy with a momentum k measured from the chemical potential μ . $c_{k,\sigma}$ is an annihilation operator of a Fermi atom with spin $\sigma = \uparrow, \downarrow$. The coupling constant U is related to the p -wave scattering length a as

$$\frac{m}{2a} = \frac{1}{U} + \sum_k \frac{\Gamma_k^2}{2\epsilon_k}, \quad (4)$$

where the form factor Γ_k is an odd function of k and $\epsilon_k = k^2/(2m)$. In this paper, we assume $\Gamma_k = O(k)$ for $|k| \rightarrow \infty$, which is justified near a p -wave resonance in 1D. Indeed, the form factor in the zero-range limit is given by $\Gamma_k = k$ for any k ^{43,49,51–53,56}, while effects of a positive effective range can be taken into account by the form factors with different shapes such as $\Gamma_k = k/(k^2\gamma^2 + 1)$ ⁵¹. We note that while the two-channel model is employed to describe p -wave Feshbach resonance with a negative effective range in higher dimensions, one can use the present single-channel model without conflicting with Wigner's causality bound in 1D^{57–59}. Also, the parameters of a transverse trapping are included in a in the case of quasi-1D systems^{60,61}.

B. BCS-Leggett theory

In a strictly 1D system, superfluid states accompanied by condensation are prohibited by the Mermin-Wagner-Hohenberg theorem^{62,63}. Nevertheless, here we set the mean-field superfluid state, provided that the quasi-1D system is concerned where weak three-dimensional properties allow us to describe the quasi-long-range ordered state within the mean-field approach. Namely, we introduce the p -wave superfluid order parameter

$$\Delta(k) = -U\Gamma_k \sum_{k'} \Gamma_{k'} \langle c_{-k'\downarrow} c_{k'\uparrow} \rangle \equiv \Gamma_k D. \quad (5)$$

By taking an appropriate gauge transformation, we can take D as a positive value without loss of generality, so that $\Delta(k)$ becomes real valued. The mean-field Hamiltonian reads

$$\begin{aligned} H_{\text{MF}} &= \sum_k \Psi_k^\dagger \begin{pmatrix} \xi_k & -\Delta(k) \\ -\Delta(k) & -\xi_k \end{pmatrix} \Psi_k - \frac{D^2}{U} + \sum_k \xi_k \\ &\equiv \sum_k \Psi_k^\dagger H_{\text{BdG}}(k) \Psi_k - \frac{D^2}{U} + \sum_k \xi_k, \end{aligned} \quad (6)$$

where $\Psi_k = (c_{k,\uparrow}, c_{-k,\downarrow}^\dagger)^\text{T}$ is the two-component Nambu spinor. Although the mean-field Hamiltonian for the spin-triplet superfluid is generally described in terms of the four-component Nambu spinors, we do not have to use the four-component one since the present system involves only the interspin p -wave pairing interaction and the off-diagonal part for the equal spin pairing ($\uparrow\uparrow$ and $\downarrow\downarrow$) is trivially zero. The Bogoliubov transformation

$$\begin{pmatrix} \alpha_{k,1} \\ \alpha_{k,2}^\dagger \end{pmatrix} = \begin{pmatrix} u_k c_{k,\uparrow} - v_k c_{-k,\downarrow}^\dagger \\ u_k c_{-k,\downarrow}^\dagger + v_k c_{k,\uparrow} \end{pmatrix} \quad (7)$$

leads to

$$H_{\text{MF}} = \sum_k \sum_{i=1,2} E_k \alpha_{k,i}^\dagger \alpha_{k,i} + E_{\text{GS}}, \quad (8)$$

where

$$E_k = \sqrt{\xi_k^2 + \Delta^2(k)} = \sqrt{\xi_k^2 + D^2 \Gamma_k^2} \quad (9)$$

is the dispersion of the Bogoliubov quasiparticle and

$$E_{\text{GS}} = -\frac{D^2}{U} + \sum_k (\xi_k - E_k) \quad (10)$$

is the ground-state energy. In Eq. (7), $u_k^2 = \frac{1}{2}(1 + \xi_k/E_k)$ and $v_k^2 = \frac{1}{2}(1 - \xi_k/E_k)$ are the BCS coherence factors. For given a and the particle number N , D and μ are determined by solving the following two equations self-consistently: The first one is the so-called gap equation,

$$\frac{m}{2a} + \sum_k \Gamma_k^2 \left[\frac{1}{2E_k} - \frac{1}{2\epsilon_k} \right] = 0, \quad (11)$$

resulting from the minimization condition of E_{GS} with respect to D , while the other one is the particle number equation

$$N = -\frac{\partial E_{\text{GS}}}{\partial \mu} = \sum_k \left[1 - \frac{\xi_k}{E_k} \right]. \quad (12)$$

Discussions of numerically evaluated D and μ are presented in Sec. IV A (see Fig. 1). We note that a mean-field theory for spin polarized Fermi atoms with p -wave interaction has been studied in a similar way⁵⁶.

C. Topological classification

Here we revisit the classification of topological superconductors/superfluids and show the symmetry class of the present system⁶⁴. The Bogoliubov-de Gennes (BdG) Hamiltonian $H_{\text{BdG}}(k)$ in Eq. (6) can be rewritten as

$$H_{\text{BdG}}(k) = \boldsymbol{\sigma} \cdot \mathbf{R}(k), \quad (13)$$

where $\boldsymbol{\sigma} = (\sigma_x, \sigma_y, \sigma_z)$ is a set of the Pauli matrices acting on the particle-hole space, and we have defined

$$\mathbf{R}(k) = (-\Delta(k), 0, \xi_k) \quad (14)$$

We note that the absence of σ_y terms in Eq. (13) results from the real-valued $\Delta(k)$. For classification of topological superfluids/superconductors, we start to check the particle-hole-like symmetry for $H_{\text{BdG}}(k)$ given by the following relation:

$$\Xi^{-1} H_{\text{BdG}}(-k) \Xi = -H_{\text{BdG}}(k) \quad (15)$$

where $\Xi = \sigma_x K$ is the charge-conjugation-like operator with $\Xi^2 = 1$ and K is a complex-conjugate operator. In addition, since $H_{\text{BdG}}(k)$ anticommutes with σ_y , $H_{\text{BdG}}(k)$ has the chiral symmetry given by

$$C^{-1} H_{\text{BdG}}(k) C = H_{\text{BdG}}(k), \quad (16)$$

where $C = i\sigma_y$ is the chiral operator. The chiral operator is related to Ξ and the time-reversal-like operator Θ as $C = \Theta \Xi$. We can find $\Theta = \sigma_z K$ and the following time-reversal-like symmetry:

$$\Theta^{-1} H_{\text{BdG}}(-k) \Theta = H_{\text{BdG}}(k). \quad (17)$$

Equations (15), (16), and (17) combined with $\Xi^2 = \Theta^2 = +1$ show that our 1D superfluid belongs to the class BDI⁶⁵. The \mathbb{Z} topological invariant characterizing this system is given by the winding number

$$\nu = \int_{-\infty}^{\infty} \frac{dk}{2\pi i} q^*(k) \frac{\partial}{\partial k} q(k), \quad (18)$$

where $q(k) = \hat{R}_z(k) - i\hat{R}_x(k)$ and $\hat{\mathbf{R}}(k) = \mathbf{R}(k)/|\mathbf{R}(k)|$. We note that the \mathbb{Z}_2 topological invariant ν_2 defined by $(-1)^{\nu_2} = \text{sgn}[\hat{R}_z(k=0)]\text{sgn}[\hat{R}_z(k \rightarrow \infty)]$ corresponds to

the parity of ν . As mentioned in Sec. II A, $\Gamma_k = \Delta(k)/D$ satisfies $\Gamma_k = O(k)$ for $k \rightarrow \infty$, leading to

$$(-1)^{\nu_2} = \text{sgn}(-\mu). \quad (19)$$

While the case of $\nu_2 = 1$, $\mu > 0$ corresponds to the mapping to the trajectory from the south pole $\hat{\mathbf{R}}(k=0) = (0, 0, -1)$ to the north pole $\hat{\mathbf{R}}(k \rightarrow \infty) = (0, 0, 1)$ with increasing $k \geq 0$, the other case ($\nu_2 = 0$, $\mu < 0$) does to the trivial trajectory, where both the starting and ending points are the north pole.

We emphasize that the above-mentioned classification of phases and the topological invariant based on the sign of μ [Eq. (19)] is valid regardless of details of a resonance such as an effective range. Since the key of the above discussion is $\Delta(k)/\xi_k \rightarrow 0$ for $|k| \rightarrow \infty$ and $|k| \rightarrow 0$ resulting from the assumptions of Γ_k , the discussion holds both in the zero-range limit and in the presence of a positive effective range. In addition, Eq. (19) is also valid in the case with a negative effective range, where the mean-field order parameter $\Delta(k)$ is proportional to k^{67-69} . Hereafter, we take the zero-range case $\Gamma_k = k$ for simplicity. In this case, we obtain $\nu_2 = \nu$. The systems with $\mu > 0$ ($\mu < 0$) has the topological invariant $\nu = 1$ ($\nu = 0$), and the \mathbb{Z}_2 topological phase transition occurs at $\mu = 0$.

III. OPTICAL SPIN TRANSPORT

In this section, we analytically evaluate the optical spin conductivity in a spin-1/2 p -wave topological superfluid at $T = 0$. On the basis of our previous paper²¹, we consider 1D fermions under a small external spin-dependent force $F_S(t)$. The corresponding perturbative Hamiltonian is given by $\delta H(t) = -\int dx F_S(t) x S(x)$, where $S(x) = [\psi_{\uparrow}^{\dagger}(x)\psi_{\uparrow}(x) - \psi_{\downarrow}^{\dagger}(x)\psi_{\downarrow}(x)]/2$ with $\psi_{\sigma}(x) = \sum_k c_{k,\sigma} e^{ikx}$ is the local spin imbalance. By monitoring the spin-selective center-of-mass motion under the external spin-dependent force $F_S(\omega)$ with the frequency ω (which is the Fourier transform of $F_S(t)$), one can measure the optical spin conductivity $\sigma^{(S)}(\omega) = \langle J_S(\omega) \rangle / \tilde{F}_S(\omega)$ where $\langle J_S(\omega) \rangle$ is the Fourier transform of the thermal average of the spin current operator $J_S(t) = \frac{d}{dt} \int dx S(x, t) x$ (see Ref.²¹ for more details). The linear response theory relates $\sigma^{(S)}(\omega)$ to the retarded response function $\chi(\omega)$ of a spin current as

$$\sigma^{(S)}(\omega) = \frac{i}{\omega_+} \left[\frac{N}{4m} + \chi(\omega) \right], \quad (20)$$

where $\omega_+ = \omega + i\eta$ with an infinitesimal positive number η . $\chi(\omega)$ is defined as

$$\chi(\omega) = -i \int_0^{\infty} dt e^{i\omega_+ t} \langle [J_S(t), J_S(0)] \rangle \quad (21)$$

and $\langle \cdots \rangle$ denotes the expectation value with respect to the ground state. The response function in the BCS-Leggett theory can be evaluated in the same way as in

the case of a 3D s -wave superfluid Fermi gas²¹:

$$\chi(\omega) = \sum_k \frac{k^4 D^2}{4m^2 E_k^2} \left(\frac{1}{\omega_+ - 2E_k} - \frac{1}{\omega_+ + 2E_k} \right). \quad (22)$$

Using Eqs. (12) and (22), one can confirm that the optical spin conductivity satisfies the f -sum rule^{21,70}

$$\int_{-\infty}^{\infty} d\omega \operatorname{Re} [\sigma^{(S)}(\omega)] = \frac{\pi}{4m} N. \quad (23)$$

Since the imaginary part of the optical spin conductivity can be expressed in terms of the real part with the Kramers-Kronig relation, we hereafter focus only on $\operatorname{Re} [\sigma^{(S)}(\omega)]$. From Eq. (20), we obtain

$$\operatorname{Re} [\sigma^{(S)}(\omega)] = \mathcal{D}_S \delta(\omega) - \frac{1}{\omega} \operatorname{Im} \chi(\omega), \quad (24)$$

where the spin Drude weight

$$\mathcal{D}_S = \pi \left[\frac{N}{4m} + \operatorname{Re} \chi(0) \right] \quad (25)$$

characterizes the sharp contribution at zero frequency. Using Eq. (22) as well as Eq. (12), one can find that the spin Drude weight in this superfluid always vanishes ($\mathcal{D}_S = 0$). Substituting Eq. (22) into the second term in Eq. (24) yields

$$\operatorname{Re} [\sigma^{(S)}(\omega)] = \sum_k \frac{\pi k^2 \Delta^2(k)}{m^2 |\omega|^3} \delta(|\omega| - 2E_k). \quad (26)$$

This equation indicates that the spectrum of $\operatorname{Re} [\sigma^{(S)}(\omega)]$ is sensitive to the shape of the quasiparticle dispersion $E_k = \sqrt{\xi_k^2 + D^2 k^2}$. In particular, $\operatorname{Re} [\sigma^{(S)}(\omega)]$ vanishes for $|\omega|$ below the spin gap $E_{\text{gap}} = \min[2E_k]$. For $\mu \geq mD^2$, E_k becomes minimum at a nonzero momentum, while, for $\mu < mD^2$, E_k monotonically increases with increasing $|k|$, leading to

$$E_{\text{gap}} = \begin{cases} 2D\sqrt{2m\mu - m^2 D^2} & \mu > mD^2 \\ 2|\mu| & \mu < mD^2 \end{cases}, \quad (27)$$

which shows that the spin gap is closed at $\mu = 0$ corresponding to the \mathbb{Z}_2 topological phase transition point.

The value of the chemical potential characterizes not only the topological phases [see Eq. (19)] but also the gap structures [Eq. (27)] in the quasiparticle dispersion. For this reason, we define three regions of μ with nonzero spin gap; (i) $\mu > mD^2$, (ii) $0 < \mu < mD^2$, and (iii) $\mu < 0$. The regions (i) and (ii) [(iii)] are in the topologically non-trivial (trivial) phase with $\nu = 1$ ($\nu = 0$), and in the region (i) [(ii) and (iii)] the superfluid has the spin gap associated with the nonzero-momentum (zero-momentum) quasiparticle excitation.

Performing the momentum summation in Eq. (26), we obtain an analytical expression of $\operatorname{Re} [\sigma^{(S)}(\omega)]$ as

$$\begin{aligned} \operatorname{Re} [\sigma^{(S)}(\omega)] &= \frac{D\theta(|\omega| - E_{\text{gap}})}{4m|\omega|^2 \sqrt{m^2 D^2 - 2m\mu + \left(\frac{|\omega|}{2D}\right)^2}} \\ &\times [\mathcal{K}_+^3(|\omega|) + \mathcal{K}_-^3(|\omega|)\theta(\mu - mD^2)\theta(2|\mu| - |\omega|)] \end{aligned} \quad (28)$$

where we have defined

$$\begin{aligned} \mathcal{K}_{\pm}^2(|\omega|) &= 2m(\mu - mD^2) \\ &\pm 2mD \sqrt{m^2 D^2 - 2m\mu + \left(\frac{|\omega|}{2D}\right)^2}. \end{aligned} \quad (29)$$

In the region (i) with $\mu > mD^2$, the spectrum of $\operatorname{Re} [\sigma^{(S)}(\omega)]$ shows the coherence peak $\operatorname{Re} [\sigma^{(S)}(\omega)] \sim 1/\sqrt{\omega - E_{\text{gap}}}$ for $\omega \rightarrow E_{\text{gap}} + 0$, while, in the regions (ii) and (iii), the conductivity monotonically vanishes in such a limit without exhibiting a coherence peak. It should be noted that the step function $\theta(|\omega| - E_{\text{gap}})$ in the numerator of Eq. (28) indicates that $\operatorname{Re} [\sigma^{(S)}(\omega)]$ vanishes below the spin gap E_{gap} given by Eq. (27). We will discuss this difference in spin conductivity spectra for various interaction strengths in the next section (see Fig. 2). In the high-frequency limit, $\operatorname{Re} [\sigma^{(S)}(\omega)]$ has the following power-law tail:

$$\lim_{\omega \rightarrow \infty} \operatorname{Re} [\sigma^{(S)}(\omega)] = \frac{C}{4(m|\omega|)^{\frac{3}{2}}}, \quad (30)$$

where $C = 2m^2 D^2$ is the p -wave contact obtained from the adiabatic theorem⁴⁹

$$\frac{\partial E_{\text{GS}}}{\partial a^{-1}} = -\frac{C}{4m}. \quad (31)$$

We examine the optical spin conductivity at the \mathbb{Z}_2 topological phase transition point with $\mu = 0$. In this case, the gapless excitation of the quasiparticle makes the spin gap in $\operatorname{Re} [\sigma^{(S)}(\omega)]$ closed. Equation (28) reduces to

$$\operatorname{Re} [\sigma^{(S)}(\omega)] = \frac{mD^3 \left[\sqrt{1 + \omega^2/(4m^2 D^4)} - 1 \right]^{3/2}}{\sqrt{2}\omega^2 \sqrt{1 + \omega^2/(4m^2 D^4)}} \quad (32)$$

for any ω . In particular, the spin conductivity linearly behaves in a small frequency region:

$$\operatorname{Re} [\sigma^{(S)}(\omega)] = \frac{|\omega|}{32m^2 D^3} + O(|\omega|^2). \quad (33)$$

We emphasize that this gapless behavior in the spectrum of the optical spin conductivity is clearly different from that of the conventional Drude-type conductivity with a sharp peak at low frequency.

IV. RESULTS AND DISCUSSIONS

A. Numerical results

Figure 1 shows the chemical potential μ and the gap parameter D along the p -wave BCS-BEC evolution obtained by solving Eqs. (11) and (12), where $k_F = \frac{\pi N}{2}$ and $E_F = \frac{k_F^2}{2m}$ are the Fermi momentum and Fermi energy of a non-interacting Fermi gas, respectively. While μ is equal

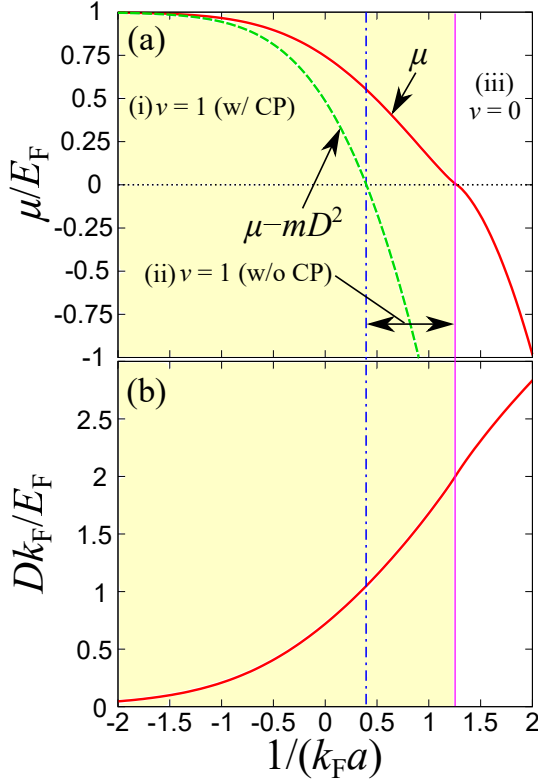


FIG. 1: Calculated (a) chemical potential μ and (b) gap parameter D along the p -wave BCS-BEC evolution with increasing the interaction strength $1/(k_F a)$. E_F and k_F are the Fermi energy and momentum, respectively. The \mathbb{Z}_2 topological phase transition occurs at $1/(k_F a) = 1.27$ where $\mu = 0$. On the other hand, the coherence peak (CP) in the optical spin conductivity disappears at $\mu - mD^2 = 0$, which is different from the 3D s -wave case where CP disappears at $\mu = 0$.

to E_F in the weak-coupling limit [$1/(k_F a) \rightarrow -\infty$], μ decreases with increasing the interaction strength $1/(k_F a)$ and finally changes its sign at $1/(k_F a) = 4/\pi = 1.27$, where the \mathbb{Z}_2 topological phase transition occurs from the non-trivial to trivial phases ($\nu = 1 \rightarrow 0$). Simultaneously, D monotonically increases with increasing $1/(k_F a)$. In contrast to μ , D does not exhibit a kink at $1/(k_F a) = 1.27$ because the absolute value of D is not important for the topological transition unless $D = 0$. These interaction dependencies of μ and D are similar to those of the s -wave BCS-BEC crossover in 3D^{71–74} (although the topological phase transition is absent in the latter case). We note that at $\mu = 0$, one can analytically solve Eqs. (11) and (12) as $D = v_F$ and $1/(k_F a) = 4/\pi$, where $v_F = k_F/m$ is the Fermi velocity. On the other hand, the region of μ with the coherence peak is different between our p -wave case and the 3D s -wave case. As shown in the previous section, $\mu > mD^2$ [the region (i)] corresponds to the case with the coherence peak for the p -wave superfluid, while $\mu > 0$ does in the 3D system^{71–74}. In Fig. 1, we also plot $\mu - mD^2$ as a function of the interaction strength and one can see that $\mu = mD^2 > 0$ is satisfied at

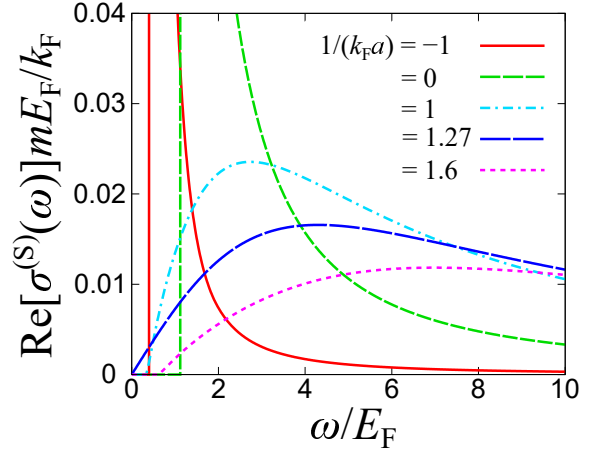


FIG. 2: Optical spin conductivity $\text{Re}[\sigma^{(S)}(\omega)]$ at various interaction strengths.

$1/(k_F a) = (4/\pi) \left[1 + 4\Gamma(\frac{5}{4})^2 / \Gamma(\frac{3}{4})^2 \right]^{-1} = 0.399$, where $\Gamma(z)$ is the gamma function.

Using Eq. (28) combined with the results of μ and D shown in Fig. 1, we plot the real part of the optical spin conductivity $\text{Re}[\sigma^{(S)}(\omega)]$ at various interaction strength in Fig. 2. In the cases of a weak coupling [$1/(k_F a) = -1$] and the p -wave unitarity [$1/(k_F a) = 0$], the system belongs to the region (i) with $\nu = 1$, and $\text{Re}[\sigma^{(S)}(\omega)]$ exhibits the spin gap and the coherence peak. On the other hand, the coherence peak in $\text{Re}[\sigma^{(S)}(\omega)]$ disappears at $1/(k_F a) = 1$ [the region (ii)]. In this case, the system remains spin gapped and has the same topological invariant ($\nu = 1$) as in the weaker coupling side. One can find the closing of the spin gap at $1/(k_F a) = 1.27$, where the \mathbb{Z}_2 topological phase transition occurs. Finally, at stronger coupling [$1/(k_F a) = 1.6$], $\text{Re}[\sigma^{(S)}(\omega)]$ shows the spin gap again, indicating that the system undergoes the topologically trivial phase, i.e., the region (iii) with $\nu = 0$.

Figure 3 shows the spin-gap energy E_{gap} in $\text{Re}[\sigma^{(S)}(\omega)]$. Indeed, one can find $E_{\text{gap}} = 0$ at $1/(k_F a) = 1.27$, where the \mathbb{Z}_2 topological phase transition occurs, and $E_{\text{gap}} > 0$ away from the transition point. By recalling the analytical form of the spin-gap energy given by Eq. (27), E_{gap} is proportional to $|\mu|$ around the transition point. Moreover, interestingly, E_{gap} exhibits a local maximum around $1/(k_F a) = 0.399$, where the coherence peak disappears (see Fig. 1). Indeed, the analytical form of E_{gap} [Eq. (27)] changes at $\mu = mD^2$. This result implies that the fermionic character of p -wave superfluidity qualitatively changes to that of the molecular bosonic condensates in this regime without any phase transitions as usual BCS-BEC crossover phenomena.

We are now in the position to examine the detailed structure of the optical spin conductivity. Figure 4 shows the frequency dependence of $\text{Re}[\sigma^{(S)}(\omega)]$ at the topological phase transition point $1/(k_F a) = 1.27$. One can confirm the linear behavior shown in Eq. (33) in the sufficiently low-frequency regime. This means that the mea-

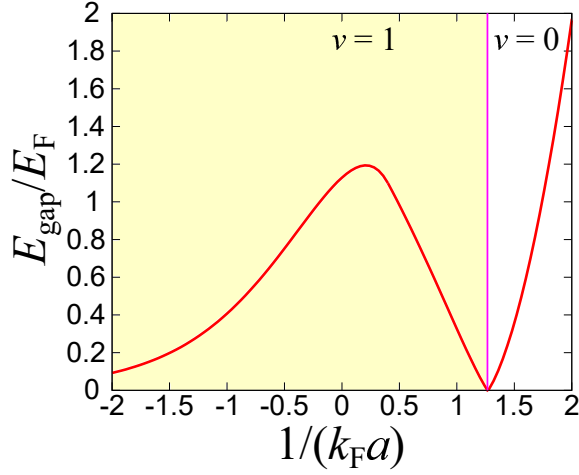


FIG. 3: Spin-gap energy E_{gap} [Eq. (27)] in the optical spin conductivity $\text{Re}[\sigma^{(S)}(\omega)]$, as a function of the interaction strength $1/(k_F a)$. The vertical line at $1/(k_F a) = 1.27$ indicates the gap-closing point accompanying the topological phase transition.

surement of the optical spin conductivity can detect the \mathbb{Z}_2 topological phase transition from the gapless behavior of $\text{Re}[\sigma^{(S)}(\omega)]$. This is analogous to the spin superfluidity at the phase boundary of the spinor Bose condensates²¹, whereas the linear spin conductivity spectra is proportional to the inverse spin velocity v_s^{-1} in this bosonic system. In the present case at $\mu = 0$, the dispersion reads

$$E_k = \sqrt{\epsilon_k^2 + D^2 k^2} = D|k| + \frac{|k|^3}{8m^2 D} + O(|k|^5), \quad (34)$$

indicating the gapless spin excitation with the spin velocity $v_s = D \equiv v_F$. Since the Drude-like conductivity is generally a decreasing function of ω in the low-frequency regime, one can clearly distinguish this gapless spectrum from the Drude one by confirming the linearly increasing behavior of $\text{Re}[\sigma^{(S)}(\omega)]$. In addition, the fact that a vanishing chemical potential results in a gapless linear behavior in $\text{Re}[\sigma^{(S)}(\omega)]$ remains correct even in the presence of the effective-range corrections. Such a low-frequency gapless behavior is in contrast to the s-wave superfluid case where $\text{Re}[\sigma^{(S)}(\omega)]$ is always gapped²¹. In the high-frequency regime, the low-energy spin excitation becomes irrelevant and $\text{Re}[\sigma^{(S)}(\omega)]$ exhibits the high-frequency tail being proportional to the p -wave contact C . The same behavior has also been reported in other systems such as the 3D s -wave unitary Fermi gas^{21,70,75} and spinor BEC²¹. We note that the high-frequency tail in $\text{Re}[\sigma^{(S)}(\omega)]$ appears in the entire p -wave BCS-BEC evolution shown in Fig. 2.

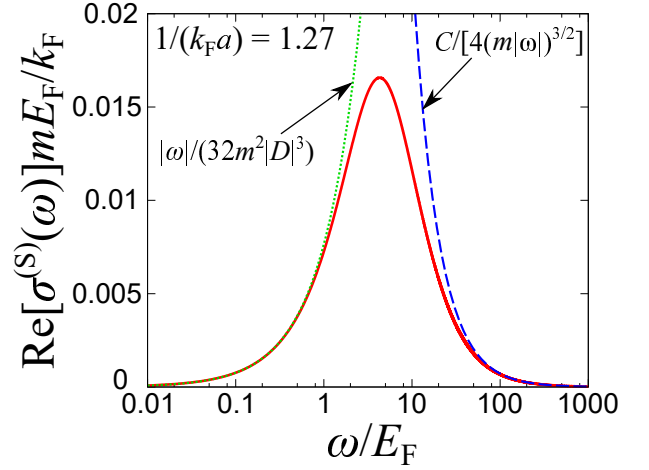


FIG. 4: The optical spin conductivity $\text{Re}[\sigma^{(S)}(\omega)]$ at the gapless point with $\mu = 0$ and $1/(k_F a) = 1.27$. The dotted and dashed lines denote the asymptotic behaviors [Eqs.(30) and (33)] at high and low frequencies, respectively.

B. Low-energy effective model for the Majorana zero mode at the edge of gas cloud

Here we consider the low-energy effective Hamiltonian for the Majorana zero mode⁷⁶ in the present spin-1/2 p -wave superfluid system. The BdG Hamiltonian in the momentum space [Eq. (13)] can be rewritten as

$$H_{\text{BdG}}(k) = Dk\sigma_x - \mu\sigma_z + O(k^2). \quad (35)$$

In this regard, the low-energy effective Hamiltonian density reads

$$\mathcal{H}_{\text{eff}}(x) = -iD(x)\sigma_x\partial_x - \mu(x)\sigma_z, \quad (36)$$

which is a Dirac Hamiltonian in $(1+1)$ dimensions, and thus the Majorana zero mode appear at $\mu(x) = 0$ ⁷⁶. While we have discussed the bulk optical spin transport, the Majorana edge state can be detected by measuring the local optical spin conductivity where the local spin-dependent drive is applied as schematically shown in Fig. 5.

Hereafter, we discuss the robustness of the low-energy effective model at p -wave unitarity even in the absence of the proximity effect, as a result of an interplay between the topological properties and the universal thermodynamics. To see this, we consider the density dependence of D and μ . At $a^{-1} = 0$, these quantities are scale invariant and exhibit

$$D \propto \frac{E_F}{k_F} \sim n^1, \quad \mu \propto E_F \sim n^2, \quad (37)$$

where $n = N/L$ is the number density. Thus, at zero density limit ($n \rightarrow 0$) corresponding to the edge region, we can safely obtain the gapless Hamiltonian at $\mu(x^*) = 0$ as

$$\mathcal{H}_{\text{eff}}(x^*) = -iD(x^*)\sigma_x\partial_x + O(n^2) \quad (38)$$

for the Majorana edge mode. Also, in the BEC side ($a^{-1} > 0$), this effective model works well since a nonzero D is obtained even at $\mu = 0$ in the bulk system. However, in such a case, the Majorana edge mode does not appear at the edge of gas cloud but it does around the dilute region of cloud where $\mu(x) = 0$ because the local density can be nonzero even for $\mu < 0$.

On the other hand, the validity of the effective Hamiltonian [Eq. (36)] is not guaranteed in the BCS side $a^{-1} < 0$. The density dependence of D and μ in the BCS side is given by

$$D \sim ne^{-\frac{1}{|a|n}}, \quad \mu \rightarrow E_F \propto n^2. \quad (39)$$

Because of non-universal effects associated with finite a , D becomes exponentially small in the dilute limit ($n \rightarrow 0$). In such a case, the decrease of D is faster than that of μ . Moreover, the higher derivative term becomes non-negligible. Although the magnitude of D around the edge region is assumed to be enough large due to the proximity effect, such an induced gap should be small in the weak-coupling regime. Therefore, we find that the low-energy description of the Majorana zero mode at the cloud edge based on Eq. (36) is more robust around the p -wave unitarity limit compared to the BCS regime. This is a special feature due to the scale invariance at p -wave unitarity.

We note that the above discussion provides the fragility of the derivative expansion given by Eq. (36) in the BCS regime. Although such an effective theory is broken down in the weak coupling regime, the existence of the Majorana zero mode would be investigated by solving the BdG equation in a similar way as for 2D trapped chiral p -wave Fermi superfluids⁷⁷.

V. SUMMARY

To summarize, we have theoretically investigated optical spin transport properties in spin-1/2 topological p -wave superfluidity in 1D, which is one of the promising candidates for realizing topological superfluid Fermi gases in recent cold atom experiments.

We have extended the BCS-Leggett theory for 3D s -wave BCS-BEC crossover phenomena to the 1D p -wave BCS-BEC evolution accompanying the \mathbb{Z}_2 topological phase transition at zero temperature. We have introduced the mean-field model Hamiltonian and how to characterize p -wave interaction with the p -wave scattering length in this system. Also, we have clarified that the present 1D continuum system belongs to the symmetry class BDI. We have found that topological characterization with chemical potential [Eq. (19)] holds not only in the zero-range limit but also in the presence of effective-range corrections.

Combining the BCS-Leggett theory and the linear response approach, we have derived the analytical formula of the optical spin conductivity along the p -wave BCS-BEC evolution. The optical spin conductivity shows the

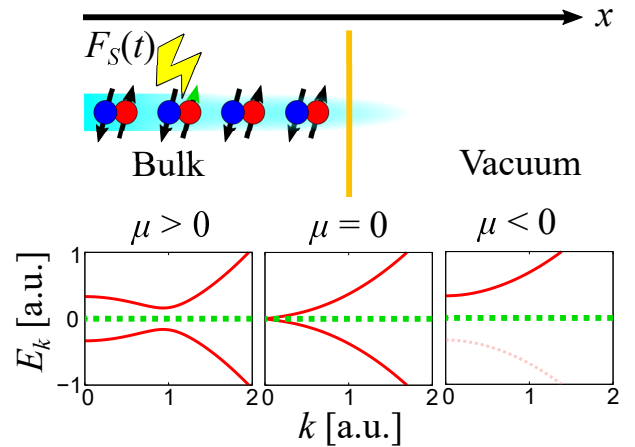


FIG. 5: Schematic figure for proving the optical spin conductivity in 1D spin-1/2 topological p -wave superfluidity. The lower panels show the energy dispersion E_K for $\mu > 0$, $\mu = 0$, and $\mu < 0$. The Majorana zero mode exits where the local chemical potential becomes zero, $\mu(x) = 0$. We note that the

negative dispersion $-E_k = -\sqrt{\left(\frac{k^2}{2m} + |\mu|\right)^2 + D^2 k^2}$ appears in the BEC side with $a^{-1} > 0$ and $\mu < 0$. Physically, this branch describes the hole-like excitation when breaking the tightly-bound p -wave molecule. Therefore, such a dispersion is absent in vacuum without two-body bound states.

spin-gapped spectrum at various interaction strengths away from the topological phase transition point with the vanishing chemical potential. On the basis of optical spin transport properties, we have classified three regimes, that is, (i) topologically non-trivial phases with the coherence peak in the BCS side, (ii) topologically non-trivial phase without the coherence peak, and (iii) topologically trivial phase in the BEC side. Moreover, the gapless linear behavior in the optical spin conductivity spectrum at the topological phase transition point is found to be distinct from the conventional Drude-type conduction. The measurement of the optical spin conductivity, therefore, can detect the topological phase transition as the closing of the spin gap. Finally, we have argued the low-energy effective Hamiltonian for the Majorana zero mode. We have showed that the scale invariance at p -wave unitarity assists the low-energy description based on the derivative expansion even in the absence of the proximity effect.

For future work, it is interesting to investigate how the gapped optical spin conductivity changes to the Drude-type conductivity at finite temperature. For instance, the spin Drude weight can be nonzero at finite temperature. The spin-gapped behavior would also remain above the superfluid critical temperature T_c due to the emergence of the pseudogap associated with pairing fluctuations. Such a many-body effect appears below the so-called pseudogap temperature T^{*74} . In addition, the theoretical framework for the optical spin conductivity can be applied to other classes of topological superconductors and superfluidity such as spin-1/2 s -wave superfluid Fermi

gas with the spin-orbit coupling^{78,79}, the p -wave superfluids in a Bose-Fermi mixture^{80,81} and the spin Hall response in higher-dimensional systems with the chiral p -wave pairing symmetry. It is worth investigating the spin conductance^{82–87} detected by the quantum point contact in topological Fermi superfluids.

Acknowledgments

The authors thank M. Matsuo, Y. Ominato and A. Fu-

rusaki for fruitful discussions. HT also thanks S. Tsutsui, T. M. Doi, and K. Iida for useful discussions in the initial stage of this study. YS is supported by JSPS KAKENHI Grants No. 19J01006. HT is supported by Grant-in-Aid for Scientific Research provided by JSPS through No. 18H05406. SU is supported by MEXT Leading Initiative for Excellent Young Researchers, JSPS KAKENHI Grant No. JP21K03436, and Matsuo Foundation.

-
- ¹ X.-L. Qi, and S.-C. Zhang, “Topological insulators and superconductors,” *Rev. Mod. Phys.* **83**, 1057 (2011).
 - ² T. Mizushima, Y. Tsutsumi, T. Kawakami, M. Sato, M. Ichioka, and K. Machida, “Symmetry-Protected Topological Superfluids and Superconductors —From the Basics to ^3He —,” *J. Phys. Soc. Jpn.* **85**, 022001 (2016).
 - ³ A. P. Mackenzi and Y. Maeno, “The superconductivity of Sr_2RuO_4 and the physics of spin-triplet pairing,” *Rev. Mod. Phys.* **75**, 657 (2003).
 - ⁴ D. J. Dean and M. Hjorth-Jensen, “Pairing in nuclear systems: from neutron stars to finite nuclei,” *Rev. Mod. Phys.* **75**, 607 (2003).
 - ⁵ M. G. Alford, A. Schmitt, K. Rajagopal, and T. Schäfer, “Color superconductivity in dense quark matter,” *Rev. Mod. Phys.* **80**, 1455 (2008).
 - ⁶ C. W. J. Beenakker, “Search for Majorana Fermions in Superconductors,” *Annu. Rev. Condens. Matter Phys.* **4**, 113 (2013).
 - ⁷ J. Sinova, S. O. Valenzuela, J. Wunderlich, C. H. Back, and T. Jungwirth, “Spin Hall effects,” *Rev. Mod. Phys.* **87**, 1213 (2015).
 - ⁸ C. L. Kane and E. J. Mele, “ \mathbb{Z}_2 Topological Order and the Quantum Spin Hall Effect,” *Phys. Rev. Lett.* **95**, 146802 (2005).
 - ⁹ S. Maekawa, S. O. Valenzuela, E. Saitoh, and T. Kimura, *Spin current* (Oxford University Press, 2012).
 - ¹⁰ B. Heinrich, Y. Tserkovnyak, G. Woltersdorf, A. Brataas, R. Urban, G. E. M. Bauer, “Dynamic Exchange Coupling in Magnetic Bilayers,” *Phys. Rev. Lett.* **90**, 187601 (2003).
 - ¹¹ G. Woltersdorf, O. Mosendz, B. Heinrich, C. H. Back, “Magnetization Dynamics due to Pure Spin Currents in Magnetic Double Layers,” *Phys. Rev. Lett.* **99**, 246603 (2007).
 - ¹² M. Matsuo, J. Ieda, K. Harii, E. Saitoh, and S. Maekawa, “Mechanical generation of spin current by spin-rotation coupling,” *Phys. Rev. B* **87**, 180402(R) (2013).
 - ¹³ H. J. Jiao and G. E. W. Bauer, “Spin Backflow and ac Voltage Generation by Spin Pumping and the Inverse Spin Hall Effect,” *Phys. Rev. Lett.* **110**, 217602 (2013).
 - ¹⁴ Y. Sun, H. Chang, M. Kabatek, Y.-Y. Song, Z. Wang, M. Jantz, W. Schneider, M. Wu, E. Montoya, B. Kardasz, B. Heinrich, S. G. E. te Velthuis, H. Schultheiss, and A. Hoffmann, “Damping in Yttrium Iron Garnet Nanoscale Films Capped by Platinum,” *Phys. Rev. Lett.* **111**, 106601 (2013).
 - ¹⁵ C. Hahn, G. de Loubens, M. Viret, O. Klein, V. V. Nale-
 - toy, and J. Ben Youssef, “Detection of Microwave Spin Pumping Using the Inverse Spin Hall Effect,” *Phys. Rev. Lett.* **111**, 217204 (2013).
 - ¹⁶ D. Wei, M. Obstbaum, M. Ribow, C. H. Back, and G. Woltersdorf, “Spin Hall voltages from a.c. and d.c. spin currents,” *Nat. Commun.* **5**, 3768 (2014).
 - ¹⁷ M. Weiler, J. M. Shaw, H. T. Nembach, and T. J. Silva, “Phase-Sensitive Detection of Spin Pumping via the ac Inverse Spin Hall Effect,” *Phys. Rev. Lett.* **113**, 157204 (2014).
 - ¹⁸ J. Li, L. R. Sheldford, P. Shafer, A. Tan, J. X. Deng, P. S. Keatley, C. Hwang, E. Arenholz, G. van der Laan, R. J. Hicken, and Z. Q. Qiu, “Direct Detection of Pure ac Spin Current by X-Ray Pump-Probe Measurements,” *Phys. Rev. Lett.* **117**, 076602 (2016).
 - ¹⁹ D. Kobayashi, T. Yoshikawa, M. Matsuo, R. Iguchi, S. Maekawa, E. Saitoh, and Y. Nozaki, “Spin Current Generation Using a Surface Acoustic Wave Generated via Spin-Rotation Coupling,” *Phys. Rev. Lett.* **119**, 077202 (2017).
 - ²⁰ Y. Kurimune, M. Matsuo, S. Maekawa, and Y. Nozaki, “Highly nonlinear frequency-dependent spin-wave resonance excited via spin-vorticity coupling,” *Phys. Rev. B* **102**, 174413 (2020).
 - ²¹ Y. Sekino, H. Tajima, and S. Uchino, “Optical Spin Transport in Ultracold Quantum Gases,” *arXiv:2103.02418 [cond-mat.quant-gas]*
 - ²² F. Schäfer, T. Fukuhara, S. Sugawa, Y. Takasu, and Y. Takahashi, “Tools for quantum simulation with ultracold atoms in optical lattices,” *Nat. Rev. Phys.* **2**, 411 (2020).
 - ²³ L. Amico, M. Boshier, G. Birkel, A. Minguzzi, C. Miniatura, L.-C. Kwek, D. Aghamalyan, V. Ahufinger, D. Anderson, N. Andrei, A. S. Arnold, M. Baker, T. A. Bell, T. Bland, J. P. Brantut, D. Cassettari, W. J. Chetcuti, F. Chevy, R. Citro, S. De Palo, R. Dumke, M. Edwards, R. Folman, J. Fortagh, S. A. Gardiner, B. M. Garraway, G. Gauthier, A. Günther, T. Haug, C. Hufnagel, M. Keil, W. von Klitzing, P. Ireland, M. Lebrat, W. Li, L. Longchambon, J. Mompart, O. Morsch, P. Naldesi, T. W. Neely, M. Olshanii, E. Orignac, S. Pandey, A. Pérez-Obiol, H. Perrin, L. Piroli, J. Polo, A. L. Pritchard, N. P. Proukakis, C. Rylands, H. Rubinsztein-Dunlop, F. Scazza, S. Stringari, F. Tosto, A. Trombettoni, N. Victorin, D. Wilkowski, K. Khani, A. Yakimenko, “State of the art and perspective on Atomtronics,” *arXiv:2008.04439*.
 - ²⁴ T. Enss and J. H. Thywissen, “Universal spin transport and quantum bounds for unitary fermions,”

- Annu. Rev. Condens. Matter Phys. **10**, 85 (2019).
- ²⁵ R. Anderson, F. Wang, P. Xu, V. Venu, S. Trotzky, F. Chevy, and J. H. Thywissen, “Conductivity Spectrum of Ultracold Atoms in an Optical Lattice,” Phys. Rev. Lett. **122**, 153602 (2019).
 - ²⁶ Y. Ohashi, “BCS-BEC Crossover in a Gas of Fermi Atoms with a p -Wave Feshbach Resonance,” Phys. Rev. Lett. **94**, 050403 (2005).
 - ²⁷ T.-L. Ho and R. B. Diener, “Fermion Superfluids of Nonzero Orbital Angular Momentum near Resonance,” Phys. Rev. Lett. **94**, 090402 (2005).
 - ²⁸ V. Gurarie, L. Radzihovsky, and A. V. Andreev, “Quantum Phase Transitions across a p -Wave Feshbach Resonance,” Phys. Rev. Lett. **94**, 230403 (2005).
 - ²⁹ C. A. Regal, C. Ticknor, J. L. Bohn, and D. S. Jin “Tuning p -Wave Interactions in an Ultracold Fermi Gas of Atoms,” Phys. Rev. Lett. **90**, 053201 (2003).
 - ³⁰ J. Zhang, E. G. M. van Kempen, T. Bourdel, L. Khaykovich, J. Cubizolles, F. Chevy, M. Teichmann, L. Tarruell, S. J. J. M. F. Kokkelmans, and C. Salomon “ P -wave Feshbach resonances of ultracold ^6Li ,” Phys. Rev. A **70**, 030702(R) (2004).
 - ³¹ Y. Inada, M. Horikoshi, S. Nakajima, M. Kuwata-Gonokami, M. Ueda, and T. Mukaiyama, “Collisional Properties of p -Wave Feshbach Molecules,” Phys. Rev. Lett. **101**, 100401 (2008).
 - ³² M. Waseem, T. Saito, J. Yoshida, and T. Mukaiyama “Two-body relaxation in a Fermi gas at a p -wave Feshbach resonance,” Phys. Rev. A **96**, 062704 (2017).
 - ³³ J. Yoshida, T. Saito, M. Waseem, K. Hattori, and T. Mukaiyama, “Scaling Law for Three-Body Collisions of Identical Fermions with p -Wave Interactions,” Phys. Rev. Lett. **120**, 133401 (2018).
 - ³⁴ M. Waseem, J. Yoshida, T. Saito, and T. Mukaiyama, “Unitarity-limited behavior of three-body collisions in a p -wave interacting Fermi gas,” Phys. Rev. A **98**, 020702(R) (2018).
 - ³⁵ M. Waseem, J. Yoshida, T. Saito, and T. Mukaiyama, “Quantitative analysis of p -wave three-body losses via cascade process,” Phys. Rev. A **99**, 052704 (2019).
 - ³⁶ D. V. Kurllov and G. V. Shlyapnikov, “Two-body relaxation of spin polarized fermions in reduced dimensionalities near a p -wave Feshbach resonance,” Phys. Rev. A **95**, 032710 (2017).
 - ³⁷ L. Zhou and X. Cui, “Stretching p -wave molecules by transverse confinements,” Phys. Rev. A **96**, 030701(R) (2017).
 - ³⁸ L. Pan, S. Chen, and X. Cui, “Many-body stabilization of a resonant p -wave Fermi gas in one dimension,” Phys. Rev. A **98**, 011603(R) (2018).
 - ³⁹ F. Fonta and K. M. O’Hara, “Experimental conditions for obtaining halo p -wave dimers in quasi-one-dimension,” Phys. Rev. A **102**, 043319 (2020).
 - ⁴⁰ Y.-T. Chang, R. Senaratne, D. Cavazos-Cavazos, and R. G. Hulet, “Collisional Loss of One-Dimensional Fermions Near a p -Wave Feshbach Resonance,” Phys. Rev. Lett. **125**, 263402 (2020).
 - ⁴¹ A. S. Marcum, F. R. Fonta, A. M. Ismail, K. M. O’Hara, “Suppression of Three-Body Loss Near a p -Wave Resonance Due to Quasi-1D Confinement,” arXiv:2007.15783 [cond-mat.quant-gas]
 - ⁴² Y. Ma and X. Cui, “Highly polarized one-dimensional Fermi gases near a narrow p -wave resonance,” Phys. Rev. A **100**, 062712 (2019).
 - ⁴³ H. Tajima, S. Tsutsui, T. M. Doi, and K. Iida “Unitary p -wave Fermi gas in one dimension,” Phys. Rev. A **104**, 023319 (2021).
 - ⁴⁴ T. Cheon and T. Shigehara, “Fermion-Boson Duality of One-Dimensional Quantum Particles with Generalized Contact Interactions,” Phys. Rev. Lett. **82**, 2536 (1999).
 - ⁴⁵ M. D. Girardeau and M. Olshanii, “Theory of spinor Fermi and Bose gases in tight atom waveguides,” Phys. Rev. A **70**, 023608 (2004).
 - ⁴⁶ S. A. Bender, K. D. Erker, and B. E. Granger, “Exponentially Decaying Correlations in a Gas of Strongly Interacting Spin-Polarized 1D Fermions with Zero-Range Interactions,” Phys. Rev. Lett. **95**, 230404 (2005).
 - ⁴⁷ M. D. Girardeau and A. Minguzzi, “Bosonization, Pairing, and Superconductivity of the Fermionic Tonks-Girardeau Gas,” Phys. Rev. Lett. **96**, 080404 (2006).
 - ⁴⁸ M. D. Girardeau and E. M. Wright, “Bright and dark solitary waves in a one-dimensional spin-polarized gas of fermionic atoms with p -wave interactions in a hard-wall trap,” Phys. Rev. A **77**, 043612 (2008).
 - ⁴⁹ X. Cui, “Universal one-dimensional atomic gases near odd-wave resonance,” Phys. Rev. A **94**, 043636 (2016).
 - ⁵⁰ Y. Sekino, S. Tan, and Y. Nishida, “Comparative study of one-dimensional Bose and Fermi gases with contact interactions from the viewpoint of universal relations for correlation functions,” Phys. Rev. A **97**, 013621 (2018).
 - ⁵¹ M. Valiente, “Bose-Fermi dualities for arbitrary one-dimensional quantum systems in the universal low-energy regime,” Phys. Rev. A **102**, 053304 (2020).
 - ⁵² M. Valiente, “Universal duality transformations in interacting one-dimensional quantum systems,” Phys. Rev. A **103**, L021302 (2021).
 - ⁵³ Y. Sekino and Y. Nishida, “Field-theoretical aspects of one-dimensional Bose and Fermi gases with contact interactions,” Phys. Rev. A **103**, 043307 (2021).
 - ⁵⁴ Z. Wu, E. Taylor, and E. Zaremba, “Probing the optical conductivity of trapped charge-neutral quantum gases,” Europhys. Lett., **110**, 26002 (2015).
 - ⁵⁵ T.-L. Ho. “Universal Thermodynamics of Degenerate Quantum Gases in the Unitarity Limit,” Phys. Rev. Lett. **92**, 090402 (2004).
 - ⁵⁶ V. Pastukhov, “Ground-state properties of dilute spinless fermions in fractional dimensions,” Phys. Rev. A **102**, 013307 (2020).
 - ⁵⁷ E. P. Wigner, “Lower Limit for the Energy Derivative of the Scattering Phase Shift,” Phys. Rev. **98**, 145 (1955).
 - ⁵⁸ H.-W. Hammer and D. Lee, “Causality and unitarity in low-energy quantum scattering,” Phys. Lett. B **681**, 500 (2009).
 - ⁵⁹ H.-W. Hammer and D. Lee, “Causality and the effective range expansion,” Ann. Phys. **325**, 2212 (2010).
 - ⁶⁰ B. E. Granger and D. Blume, “Tuning the Interactions of Spin-Polarized Fermions Using Quasi-One-Dimensional Confinement,” Phys. Rev. Lett. **92**, 133202 (2004).
 - ⁶¹ L. Pricoupenko, “Resonant Scattering of Ultracold Atoms in Low Dimensions,” Phys. Rev. Lett. **100**, 170404 (2008).
 - ⁶² N. D. Mermin and H. Wagner, “Absence of Ferromagnetism or Antiferromagnetism in One- or Two-Dimensional Isotropic Heisenberg Models,” Phys. Rev. Lett. **17**, 1307 (1966).
 - ⁶³ P. C. Hohenberg, “Existence of Long-Range Order in One and Two Dimensions,” Phys. Rev. **158**, 383 (1967).
 - ⁶⁴ M. Sato and Y. Ando, “Topological superconductors: a

- review,” Rep. Prog. Phys. **80** 076501 (2017).
- ⁶⁵ A. P. Schnyder, S. Ryu, A. Furusaki, and A. W. W. Ludwig, “Classification of topological insulators and superconductors in three spatial dimensions,” Phys. Rev. B **78**, 195125 (2008).
 - ⁶⁶ A. Y. Kitaev, “Unpaired Majorana fermions in quantum wires,” Phys.-Usp. **44**, 131 (2001).
 - ⁶⁷ Y. Ohashi, “BCS-BEC Crossover in a Gas of Fermi Atoms with a p-Wave Feshbach Resonance,” Phys. Rev. Lett. **94**, 050403 (2005).
 - ⁶⁸ V. Gurarie, L. Radzihovsky, and A. V. Andreev, “Quantum Phase Transitions across a p-Wave Feshbach Resonance,” Phys. Rev. Lett. **94**, 230403 (2005).
 - ⁶⁹ V. Gurarie, L. Radzihovsky, “Resonantly paired fermionic superfluids,” Ann. Phys. (N.Y.) (**322**), **2** (2007).
 - ⁷⁰ T. Enss, “Shear viscosity and spin sum rules in strongly interacting Fermi gases,” Eur. Phys. J. Special Topics **217**, 169 (2013).
 - ⁷¹ “The BCS-BEC Crossover and the Unitary Fermi Gas,” edited by W. Zwerger, Lecture Notes in Physics Vol. 836 (Springer, Berlin, 2012).
 - ⁷² M. Randeria and E. Taylor, “Crossover from Bardeen-Cooper-Schrieffer to Bose-Einstein Condensation and the Unitary Fermi Gas,” Annu. Rev. Condens. Matter Phys. **5**, 209 (2014).
 - ⁷³ G. C. Strinati, P. Pieri, G. Röpke, P. Schuck, and M. Urban, “The BCS-BEC crossover: From ultra-cold Fermi gases to nuclear systems,” Phys. Rep. **738**, 3 (2018).
 - ⁷⁴ Y. Ohashi, H. Tajima, and P. van Wyk, “BCS-BEC crossover in cold atomic and in nuclear systems,” Prog. Part. Nucl. Phys. **111**, 103739 (2020).
 - ⁷⁵ T. Enss and R. Haussmann, “Quantum Mechanical Limitations to Spin Diffusion in the Unitary Fermi Gas,” Phys. Rev. Lett. **109**, 195303 (2012).
 - ⁷⁶ M. Sato and S. Fujimoto “Majorana Fermions and Topology in Superconductors,” J. Phys. Soc. Jpn. **85**, 072001 (2016).
 - ⁷⁷ T. Mizushima, M. Ichioka, and K. Machida “Role of the Majorana Fermion and the Edge Mode in Chiral Superfluidity near a p-Wave Feshbach Resonance,” Phys. Rev. Lett. **101**, 150409 (2008).
 - ⁷⁸ M. Sato, Y. Takahashi, and S. Fujimoto, “Non-Abelian Topological Order in s-Wave Superfluids of Ultracold Fermionic Atoms,” Phys. Rev. Lett. **103**, 020401 (2009).
 - ⁷⁹ L. A. Toikka, “Non-Abelian Majorana fermions in topological s-wave Fermi superfluids,” New J. Phys. **21**, 113033 (2019).
 - ⁸⁰ Z. Wu and G. M. Bruun, “Topological Superfluid in a Fermi-Bose Mixture with a High Critical Temperature,” Phys. Rev. Lett. **117**, 245302 (2016).
 - ⁸¹ C. Zhu, L. Chen, H. Hu, X.-J. Liu, and H. Pu, “Spin-exchange-induced exotic superfluids in a Bose-Fermi spinor mixture,” Phys. Rev. A **100**, 031602(R) (2019).
 - ⁸² M. Lebrat, S. Häusler, P. Fabritius, D. Husmann, L. Corman, and T. Esslinger “Quantized Conductance through a Spin-Selective Atomic Point Contact,” Phys. Rev. Lett. **123**, 193605 – Published 8 November 2019
 - ⁸³ Y. Sekino, H. Tajima, and S. Uchino, “Mesoscopic spin transport between strongly interacting Fermi gases,” Phys. Rev. Research **2**, 023152 (2020).
 - ⁸⁴ S. Nakada, S. Uchino, and Y. Nishida, “Simulating quantum transport with ultracold atoms and interaction effects,” Phys. Rev. A **102**, 031302(R) (2020).
 - ⁸⁵ G. Del Pace, W. J. Kwon, M. Zaccanti, G. Roati, and F. Scazza, “Tunneling Transport of Unitary Fermions across the Superfluid Transition,” Phys. Rev. Lett. **126**, 055301 (2021).
 - ⁸⁶ K. Ono, T. Higomoto, Y. Saito, S. Uchino, Y. Nishida, and Y. Takahashi, “Observation of spin-space quantum transport induced by an atomic quantum point contact,” arXiv:2104.08766 [cond-mat.quant-gas]
 - ⁸⁷ Y. Ominato, A. Yamakage, M. Matsuo, “Anisotropic Superconducting Spin Transport at Magnetic Interfaces,” arXiv:2103.05871[cond-mat.supr-con]